Supporting information:

Conformationally regulated peptide bond cleavage in bradykinin

Daniel R. Fuller,[†] Christopher R. Conant,[†] Tarick J. El-Baba,[†] Christopher J. Brown,[†] Daniel W. Woodall,[†] David H. Russell,[‡] and David E. Clemmer[†,*]

[†]*Department of Chemistry, Indiana University, Bloomington, IN 47405, United States*

[‡]*Department of Chemistry, Texas A&M University, College Station, TX 77842, United States*

Correspondence to: clemmer@indiana.edu

Experimental

Sample Preparation. Bradykinin (BK, ≥98% purity) was purchased from Sigma-Aldrich (St. Louis, MO, U.S.A.). BK was prepared in water, methanol, ethanol, and 1-propanol (see Figure S3 for more details). 1 mM stock solutions of BK were diluted to 5 μM prior to analysis. Additionally, 0.5% acetic acid was added to the sample.

Temperature controlled electrospray ionization source. In order to maintain our spray temperature at the incubation temperature, a temperature-controlled electrospray ionization (ESI) source, described in detail previously,[1] and based on earlier designs,[2-4] was interfaced to the instrument. Solution is pushed through silica capillary into a stainless steel capillary connected to ESI emitter with a small inner diameter (5-15 μM) which has been laser pulled using a Sutter P2000 Tip Puller (Sutter Instruments, Novato, Ca). The capillary is housed in an aluminum block seated on a sheet of ceramic atop a thermoelectric heater/cooler (TE Tech Traverse City, MI). The ESI source allows us to control the temperature of our electrospray solution within 1 °C.

Instrumentation. Experiments were performed on a home-built 2-meter drift tube ion mobility spectrometer coupled to a time-of-flight mass spectrometer described in detail previously. [5-6] Positively charged ions are produced by electrospray ionization and accumulated in the instrument source before being periodically pulsed into the drift tube, where they are separated based on their mobilities. The drift tube is operated with ~3 torr He buffer gas and a weak electric field (~10 $V \cdot cm^{-1}$). The ions exit the drift tube and are orthogonally pulsed into a time-of-flight mass spectrometer for mass analysis. The drift times of the ions can be converted to a collision cross section (Ω, in $Å^2$) according to the following equation:[7]

$$\Omega = \frac{(18\pi)^{1/2}}{16}\frac{ze}{(k_b T)^{1/2}}\left[\frac{1}{m_I}+\frac{1}{m_B}\right]^{1/2}\frac{t_D E}{L}\frac{760}{P}\frac{T}{273.2}\frac{1}{N}$$

where *ze* is the charge of the ion, k_b is Boltzmann's constant, m_I is the mass of the ion, m_B is the mass of the buffer gas, t_D is the experimentally measured drift time, *E* is the electric field, *L* is the drift tube length, *T* is the temperature, *P* is the pressure, and *N* is the neutral number density of the gas at STP.

In order to confirm the identity of the $[BK_{(3-9)}]^{2+}$ product, we infused the BK solution after it had reacted for 120 min at 75 °C on a Waters Synapt G2S instrument and acquired tandem MS/MS on the species of interest. Quadrupole isolated $[BK_{(3-9)}]^{2+}$ ions (m/*z* = 404.22) were fragmented following ion mobility separation. Peptide sequencing was completed manually using the $BK_{(3-9)}$ sequence and are shown if Figure S2.

Cis/trans assignments for the conformations of $[BK+2H]^{2+}$. *Cis/trans* assignments of the prolines for doubly charged BK were done by substituting out proline for alanine. Where proline can readily adopt both *cis* and *trans* orientations, alanine exists almost entirely in the *trans* orientation. Since alanine has a smaller intrinsic size parameter, its contribution to the overall cross section of the peptide is less than that of proline.[8-9] Therefore, we correct the measured cross section value based on the intrinsic size difference between proline and alanine. Figure S3 shows MS data for each of the three prolines substituted for alanine. After adjustment of the cross sections, we can gain insight into the *cis*/*trans* orientations of the prolines for each of the conformations observed. Substitution of the first two prolines gives us a clear picture that Pro^2 and Pro^3 for the two conformations are; *trans*-Pro^2, *trans*-Pro^3 for the more compact conformation, and *trans*-Pro^2, *cis*-Pro^3 for the dominant, more extended conformation. However, the assignment for Pro^7 is not unambiguous. We assigned it as *cis*-Pro^7 for both conformations due to the low signal, suggesting the bond is not favored in the *trans* configuration, and because the peaks do not line up after cross section adjustment to the native $[BK+2H]^{2+}$ conformations.

Kinetics Experiments. Solutions of BK were incubated in a water bath at six different temperatures (55, 60, 65, 70, 75, and 78 °C). Figure S4 shows the data from the other temperatures of BK not shown in the main text. Bradykinin stock solutions were kept at -20 °C prior to use in order to prevent any premature degradation. Aliquots were periodically taken from the vials in the water bath at different times during the dissociation reaction and analyzed immediately. Both collision cross section and m/z distributions were followed as the dissociation progressed. Individual peak areas from the mass spectra were integrated in OriginPro 2016 (OriginLab Corporation, Northampton, MA) along with the individual conformer areas in each collision cross section distribution found in $[BK+2H]^{2+}$, $[BK+3H]^{3+}$, and $[BK_{(3-9)}+2H]^{2+}$ (since the fragments observed are complementary, $[BK_{(3-9)}+2H]^{2+}$ and $[Arg^{1}\text{-}Pro^{2}+H]^{+}$, we only integrate one of the fragment areas); each datapoint was normalized to the total ion signal in a respective mass spectrum. While the focus of this work was the dissociation of BK in ethanol, we note that the dissociation occurs in other solutions demonstrated by representative MS shown in Figure S5.

Determination of the rate constants for the reaction were performed by solving a series of first-order differential rate equations using Maple 2016.0 software; many models were iteratively and rigorously tested. The solutions to each candidate mechanism were fit to the experimental data by optimizing the rate constants using user-defined programs written in OriginPro 2016 software. Figure S6 shows all the models tested. The goodness of fit was determined by plotting the sum of residual sum of squares for each model (Figure 3 main text); identification of minima in these plots provides a means for evaluating the goodness of fit for each mechanism.

Effect of acetic acid. We focus these studies on solutions containing a small amount of acid. Addition of acetic acid makes us sensitive to all the products of this reaction, stabilizes the

ion signals, and suppresses adduct formation associated with trace contaminants. Similar to previous results,[10] there is no strong evidence that the concentration of acetic acid influences the rate of dissociation (Figure S7).

Determination of Arrhenius activation parameters. The Arrhenius equation establishes a relationship between the rate constant (k) and temperature (T),

$$k = Ae^{\frac{-E_a}{RT}}$$

where k is the rate constant, E_a is the activation barrier, A is the pre-exponential factor and R is the universal gas constant. Arrhenius activation parameters can be determined by performing a linear regression on the data points in plots of ln(k) vs. 1/T. From the slope and intercept of these plots, one can determine E_a and A for each step in the transition. Thermodynamic activation parameters (enthalpy of activation ($\Delta H^{\ddagger}$), entropy of activation ($\Delta S^{\ddagger}$) and Gibbs free energy($\Delta G^{\ddagger}$)) can be derived from the following equations:

$$\Delta H^{\ddagger} = E_a - RT$$

$$A = \frac{k_B T}{h} e^{\frac{\Delta S^{\ddagger}}{R}}$$

$$\Delta G^{\ddagger} = \Delta H^{\ddagger} - T\Delta S^{\ddagger}$$

where h is Planck's constant. Figure S8 shows the Arrhenius plots for the mechanisms shown in main text in Figure 3.

Figure Captions

Figure S1: Diagram of temperature-controlled ESI source.

Figure S2. Tandem MS/MS spectrum showing the fragmented $[BK_{(3-9)}]^{2+}$ species. BK solution was infused after 120 min reaction at 75 °C in an ethanol solution with 0.5% acetic acid. Data were acquired on isolated precursor following ion mobility separation at a collision energy of 27 V. Characteristic fragment ions are labeled in the mass spectrum. Furthermore, we overlay the peptide sequence with the main b- and y-series ions.

Figure S3. IMS data for alanine substitutions of the three prolines for $[BK+2H]^{2+}$. The proline substituted is labeled on the right side of each plot. Cross sections were adjusted based on the intrinsic size difference between alanine and proline.

Figure S4. Dissociation data acquired at four temperatures; 55, 60, 70, 75, and 78 °C. $BK(2H^+)$ is shown as squares, $BK(3H^+)$ as open circles, and $BK_{(3-9)}(2H^+)$ as triangles.

Figure S5. Comparison of dissociation of BK in solutions of 1-propanol, ethanol, methanol, and water, all with 0.5% acetic acid at 150 min and 65 °C. In each solution we observe formation of $BK_{(3-9)}(2H^+)$ at increasing abundances in the order, water, methanol, ethanol, and 1-propanol, respectively.

Figure S6. All mechanisms tested for the dissociation of BK. Mechanisms are ordered by increasing number of intermediates, with their goodness of fit (∑RSS value) located in Figure 3, main text. In some mechanisms we combined all conformations within a charge state (i.e. for

BK($2H^+$), areas of TTC($2H^+$) and TCC($2H^+$) are added together), whereas other mechanisms we parse out the individual conformer areas.

Figure S7. Abundance of intact BK vs. time at two different acid concentrations (0.5%, 2.5%).

Figure S8. Arrhenius plots shown for the two mechanisms mentioned in the main text (pathway 1, left; pathway 2, right). Step 1 is in pink, step 2 in orange, step 3 in green, step 4 in dark red, and step 5 in blue.

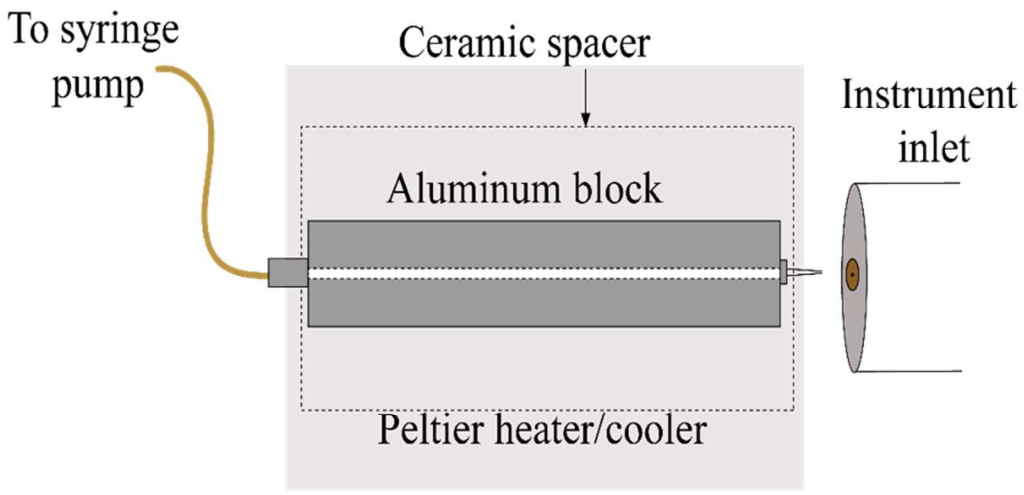
To syringe pump
Ceramic spacer
Instrument inlet
Aluminum block
Peltier heater/cooler

Figure S1.

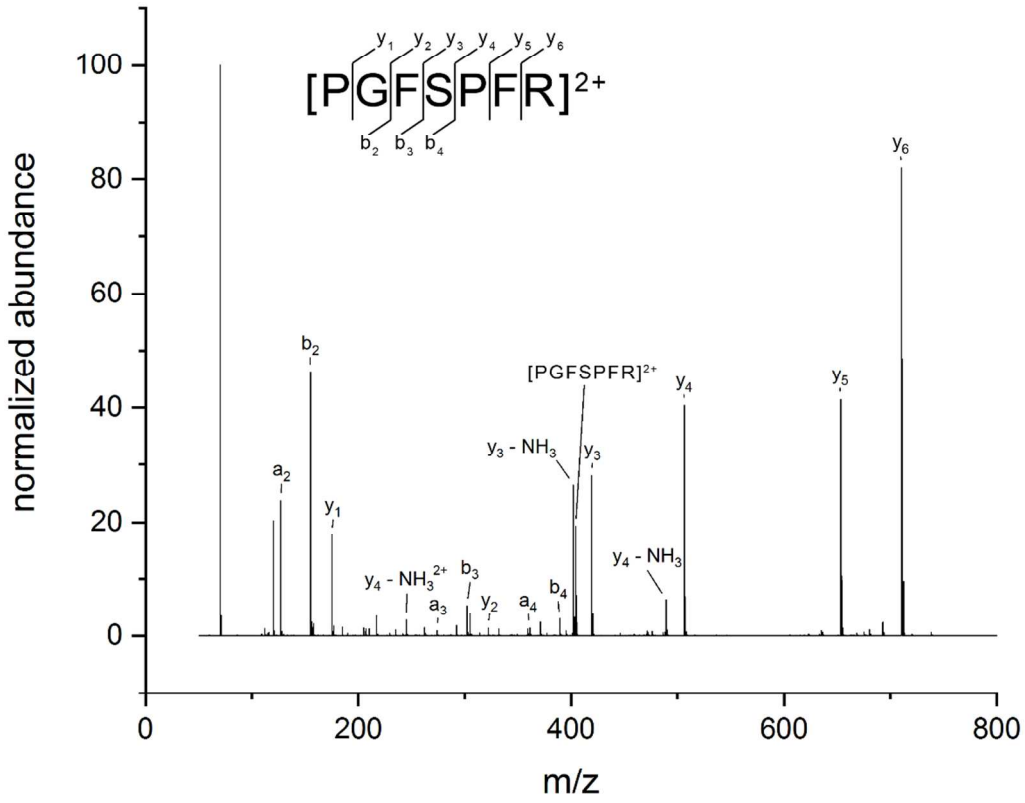
[PGFSPFR]2+
y1 y2 y3 y4 y5 y6
b2 b3 b4
normalized abundance
m/z
0
20
40
60
80
100
0
200
400
600
800
b2
a2
y1
y4 - NH3 2+
a3
b3
y2
a4
b4
[PGFSPFR]2+
y3 - NH3
y3
y4
y4 - NH3
y5
y6

Figure S2.

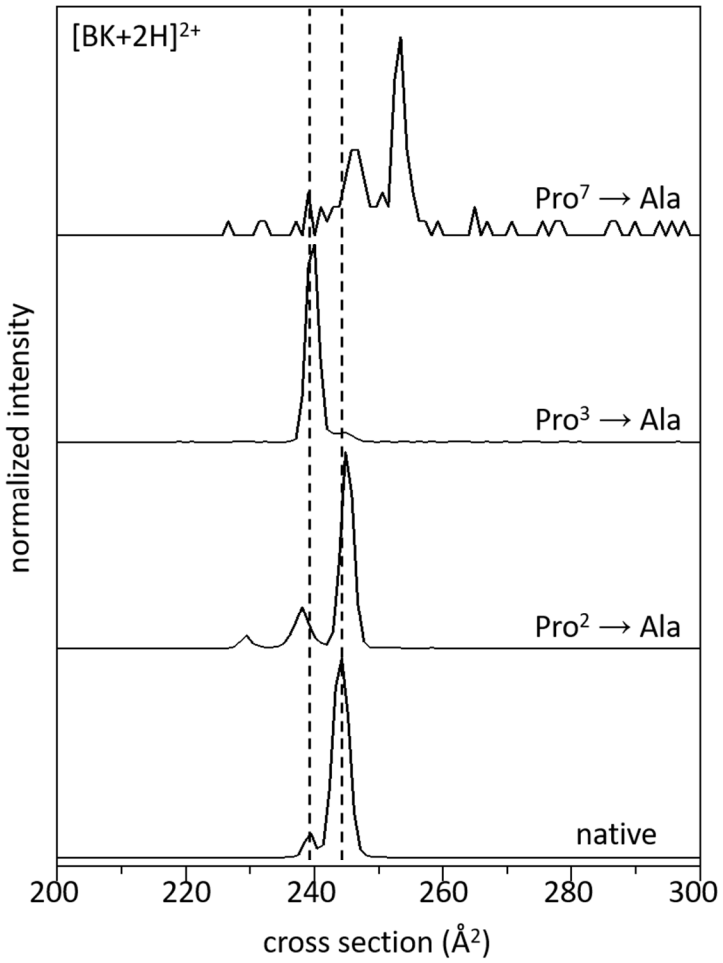
[BK+2H]2+
Pro7 → Ala
Pro3 → Ala
Pro2 → Ala
native
normalized intensity
200
220
240
260
280
300
cross section (Å2)

Figure S3.

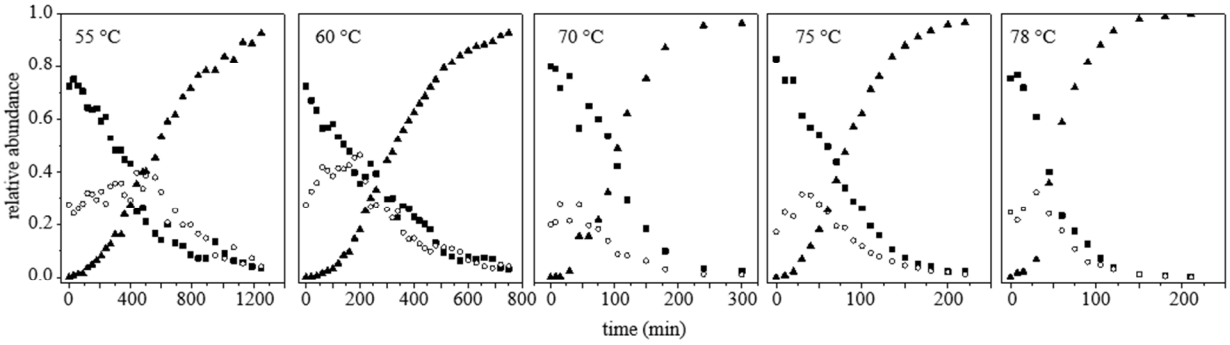

Figure S4.

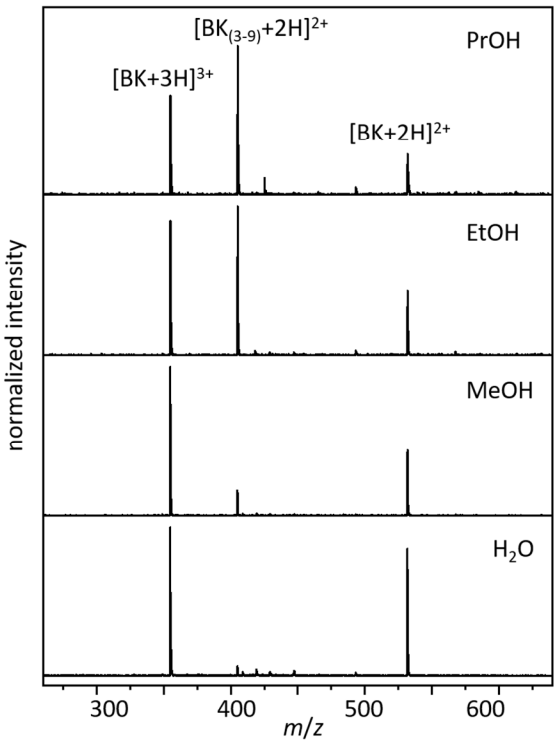
[BK(3-9)+2H]2+
PrOH
[BK+3H]3+
[BK+2H]2+
EtOH
MeOH
H2O
normalized intensity
300
400
500
600
m/z

Figure S5.

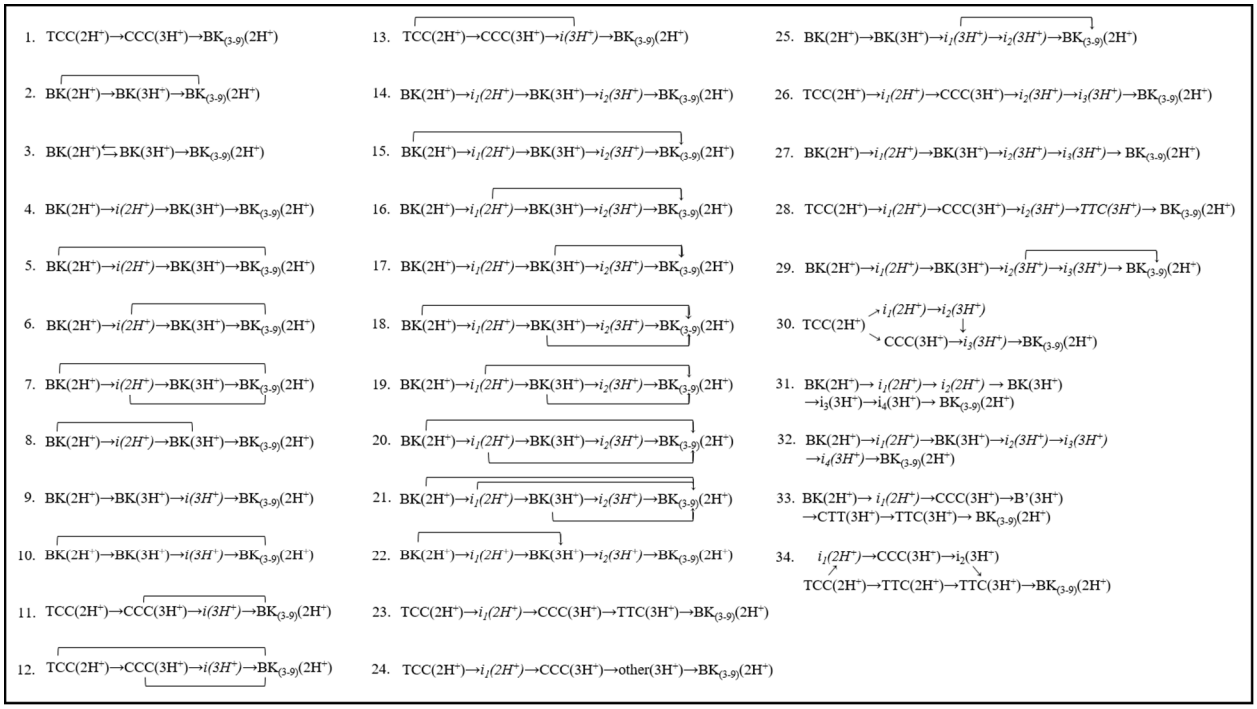
1. TCC(2H+)→CCC(3H+)→BK(3-9)(2H+)
2. BK(2H+)→BK(3H+)→BK(3-9)(2H+)
3. BK(2H+)⇆BK(3H+)→BK(3-9)(2H+)
4. BK(2H+)→i(2H+)→BK(3H+)→BK(3-9)(2H+)
5. BK(2H+)→i(2H+)→BK(3H+)→BK(3-9)(2H+)
6. BK(2H+)→i(2H+)→BK(3H+)→BK(3-9)(2H+)
7. BK(2H+)→i(2H+)→BK(3H+)→BK(3-9)(2H+)
8. BK(2H+)→i(2H+)→BK(3H+)→BK(3-9)(2H+)
9. BK(2H+)→BK(3H+)→i(3H+)→BK(3-9)(2H+)
10. BK(2H+)→BK(3H+)→i(3H+)→BK(3-9)(2H+)
11. TCC(2H+)→CCC(3H+)→i(3H+)→BK(3-9)(2H+)
12. TCC(2H+)→CCC(3H+)→i(3H+)→BK(3-9)(2H+)
13. TCC(2H+)→CCC(3H+)→i(3H+)→BK(3-9)(2H+)
14. BK(2H+)→i1(2H+)→BK(3H+)→i2(3H+)→BK(3-9)(2H+)
15. BK(2H+)→i1(2H+)→BK(3H+)→i2(3H+)→BK(3-9)(2H+)
16. BK(2H+)→i1(2H+)→BK(3H+)→i2(3H+)→BK(3-9)(2H+)
17. BK(2H+)→i1(2H+)→BK(3H+)→i2(3H+)→BK(3-9)(2H+)
18. BK(2H+)→i1(2H+)→BK(3H+)→i2(3H+)→BK(3-9)(2H+)
19. BK(2H+)→i1(2H+)→BK(3H+)→i2(3H+)→BK(3-9)(2H+)
20. BK(2H+)→i1(2H+)→BK(3H+)→i2(3H+)→BK(3-9)(2H+)
21. BK(2H+)→i1(2H+)→BK(3H+)→i2(3H+)→BK(3-9)(2H+)
22. BK(2H+)→i1(2H+)→BK(3H+)→i2(3H+)→BK(3-9)(2H+)
23. TCC(2H+)→i1(2H+)→CCC(3H+)→TTC(3H+)→BK(3-9)(2H+)
24. TCC(2H+)→i1(2H+)→CCC(3H+)→other(3H+)→BK(3-9)(2H+)
25. BK(2H+)→BK(3H+)→i1(3H+)→i2(3H+)→BK(3-9)(2H+)
26. TCC(2H+)→i1(2H+)→CCC(3H+)→i2(3H+)→i3(3H+)→BK(3-9)(2H+)
27. BK(2H+)→i1(2H+)→BK(3H+)→i2(3H+)→i3(3H+)→ BK(3-9)(2H+)
28. TCC(2H+)→i1(2H+)→CCC(3H+)→i2(3H+)→TTC(3H+)→ BK(3-9)(2H+)
29. BK(2H+)→i1(2H+)→BK(3H+)→i2(3H+)→i3(3H+)→ BK(3-9)(2H+)
30. TCC(2H+) → i1(2H+)→i2(3H+) ↓ CCC(3H+)→i3(3H+)→BK(3-9)(2H+)
31. BK(2H+)→ i1(2H+)→ i2(2H+) → BK(3H+) →i3(3H+)→i4(3H+)→ BK(3-9)(2H+)
32. BK(2H+)→i1(2H+)→BK(3H+)→i2(3H+)→i3(3H+) →i4(3H+)→BK(3-9)(2H+)
33. BK(2H+)→ i1(2H+)→CCC(3H+)→B'(3H+) →CTT(3H+)→TTC(3H+)→ BK(3-9)(2H+)
34. i1(2H+)→CCC(3H+)→i2(3H+) ↘ TCC(2H+)→TTC(2H+)→TTC(3H+)→BK(3-9)(2H+)

Figure S6.

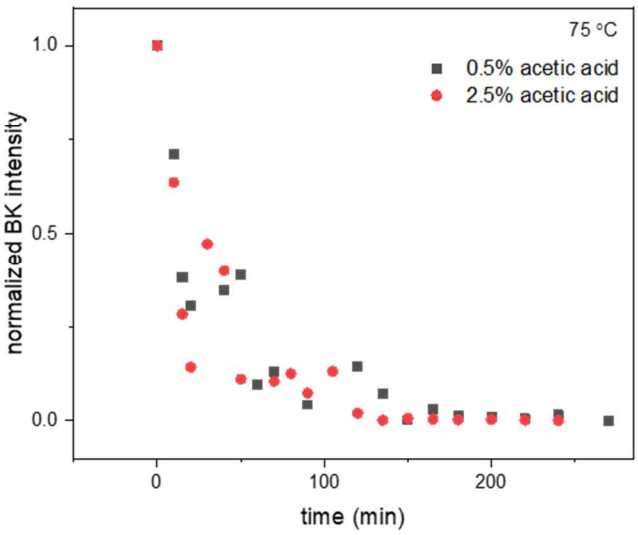
75 °C
0.5% acetic acid
2.5% acetic acid
normalized BK intensity
1.0
0.5
0.0
0
100
200
time (min)

Figure S7.

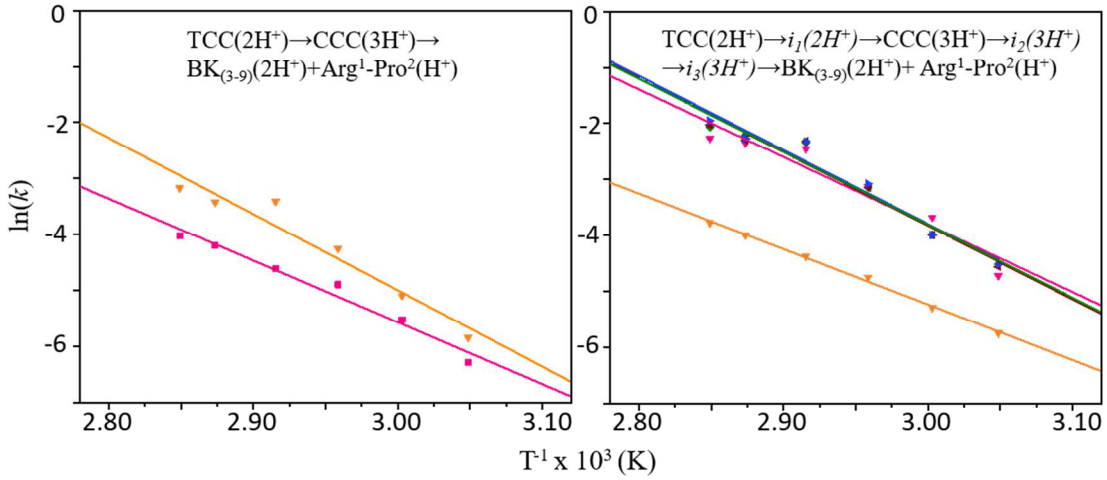
TCC(2H+)→CCC(3H+)→
BK(3-9)(2H+)+Arg1-Pro2(H+)
TCC(2H+)→i1(2H+)→CCC(3H+)→i2(3H+)
→i3(3H+)→BK(3-9)(2H+)+ Arg1-Pro2(H+)
ln(k)
0
-2
-4
-6
2.80
2.90
3.00
3.10
T-1 x 10³ (K)

Figure S8.

References.

1. El-Baba, T. J.; Woodall, D. W.; Raab, S. A.; Fuller, D. R.; Laganowsky, A.; Russell, D. H.; Clemmer, D. E. *J. Am. Chem. Soc.* **2017**, *139*, 6306-6309.
2. Benesch, J. L.; Sobott, F.; Robinson, C. V. *Anal. Chem.* **2003,** *75*, 2208-2214.
3. Wang, G.; Abzalimov, R. R.; Kaltashov, I. A. *Anal. Chem.* **2011,** *83*, 2870-2876.
4. Cong, X.; Liu, Y.; Liu, W.; Liang, X.; Russell, D. H.; Laganowsky, A. *J. Am. Chem. Soc.* **2016,** *138*, 4346-4349.
5. Koeniger, S. L.; Merenbloom, S. I.; Valentine, S. J.; Jarrold, M. F.; Udseth, H. R.; Smith, R. D.; Clemmer, D. E. *Anal. Chem.* **2006,** *78*, 4161-4174.
6. Merenbloom, S. I.; Koeniger, S. L.; Valentine, S. J.; Plasencia, M. D.; Clemmer, D. E. *Anal. Chem.* **2006,** *78*, 2802-2809.
7. Mason, E. A.; McDaniel, E. W. *Transport properties of ions in gases*. Wiley: New York, NY, 1988.
8. Valentine, S. J.; Counterman, A. E.; Hoaglund-Hyzer, C. S.; Clemmer, D. E. *J. Phys. Chem. B* **1999,** *103*, 1203-1207.
9. Srebalus Barnes, C. A.; Clemmer, D. E. *J. Phys. Chem. A* **2003,** *107*, 10566-10579.
10. Shi, L.; Holliday, A. E.; Khanal, N.; Russell, D. H.; Clemmer, D. E. *J. Am. Chem. Soc.* **2015,** *137*, 8680-8683.